SCIENCE CHINA
Information Sciences

• RESEARCH PAPERS •
Special Focus

July 2010 Vol. 53 No. 7: 1287–1295
doi: 10.1007/s11432-010-4005-x

Cubic surface fitting to image by combination

LI XueMei[1], ZHANG CaiMing[1,2]*, YUE YiZhen[1] & WANG KunPeng[1]

[1]*School of Computer Science and Technology, Shandong University, Jinan* 250101*, China;*
[2]*School of Computer Science and Technology, Shandong Economics University, Jinan* 250014*, China*

Received November 9, 2009; accepted February 21, 2010

Abstract We present a new method for constructing a fitting surface to image data. The new method is based on a supposition that the given image data are sampled from an original scene that can be represented by a surface defined by piecewise quadratic polynomials. The surface representing the original scene is known as the original surface in this paper. Unlike existing methods, which generally construct the fitting surface to the original surface using image data as interpolation data, the new method constructs the fitting surface using the image data as constraints to reverse the sampling process, which improves the approximation precision of the fitting surface. Associated with each data point and its near region, the new method constructs a quadratic polynomial patch locally using the sampling formula as constraint. The quadratic patch approximates the original surface with a quadratic polynomial precision. The fitting surface which approximates the original surface is formed by the combination of all the quadratic polynomial patches. The experiments demonstrate that compared with Bi-cubic and Separable PCC methods, the new method produced resized images with high precision and good quality.

Keywords surface fitting, quadratic polynomial, image resizing, reversing

Citation Li X M, Zhang C M, Yue Y Z. Cubic surface fitting to image by combination. Sci China Inf Sci, 2010, 53: 1287–1295, doi: 10.1007/s11432-010-4005-x

1 Introduction

The problem of resizing an image is of fundamental importance in the fields such as computer graphics and image processing [1]. This problem arises frequently whenever a user wishes to get a better view of a given image. For example, the techniques of image resizing are often required in real applications, such as image-processing, image database, medical imaging, and so on. This paper addresses the problem of constructing a fitting surface for the image data points to improve the precision and quality of the resized image.

Usually, the image resizing is done by interpolating the discrete source image. The simplest interpolation method for resizing image is pixel replication. Higher precision methods include bilinear interpolation [2, 3] and bi-cubic interpolation [4–8]. Pixel replication method is the nearest neighbor interpolation, which is easy to implement. The interpolation precision of this method is a constant, and hence results in the usually undesirable defects of blocking effects. Bilinear and bi-cubic interpolations use polynomials of degree one and three respectively, which make the resized image more visually pleasing than the replication method does. Besides, some other types of interpolation methods, such as Least-Square

*Corresponding author (email: czhang@sdu.edu.cn)

based [9], fractal-based [10] and B-spline-based [11] are also attracting research interest. These methods also achieve encouraging improvements over the traditional linear and cubic techniques. For the methods of resizing medical image, one can find them in a survey [12]. Battiato et al. [13] proposed a locally adaptive resizing algorithm, which is superior to pixel replication and bilinear interpolations in terms of quality. However, the implementation of the algorithm is complicated. Chang et al. [14] proposed an image resizing method based on the vector quantization approximation for magnifying gray-scale and color images by a factor of 2. The unknown pixel values on the image are interpolated by using a vector quantization codebook based on their local information. Therefore, the magnified images can be decoded easily and quickly from the trained codebook. Reichenbach and Shi [15, 16] presented a method of piecewise cubic convolution for image interpolation. The method seems better than the traditional separable piecewise cubic convolution method. Li and Orchard [17] proposed an edge-directed interpolation algorithm. The interpolation is adapted by the local covariance and a solution is provided to estimate the high-resolution covariance from the low-resolution counterpart based on their geometric duality. Recently, Zhang and Wu [18] developed a soft-decision interpolation method which estimated missing pixels in group rather than one pixel at a time. Generally speaking, these interpolation methods [1–18] are based on the sampling data points on a region of the image, so many details of the image will be lost.

Avidan and Shamir [19, 20] recently studied new methods for content-aware image resizing. Rather than cropping, they adjusted the image size by adding or removing seams, where the dynamic programming is used to find seams. The advantage of the methods is that they will not cause obvious distortion when changing the aspect ratio. But the methods are slow, as dynamic programming is used. Another work by Zhang [21] examined the shrinkability of each pixel and achieved good results for video resizing, however, the construction of shrinkability map is not so efficient for real time applications. Huang et al. [22] gave a fast content-aware resizing algorithm. The main contribution is that a novel approach is provided to make the algorithm efficient, the results comparable to those of Avidan and Shamir's methods [19, 20].

In this paper, we propose a new method for constructing the fitting surface to image data. The new method supposes that the given data points of an image are sampled from an original scene that can be represented by a surface known as the original surface. Based on the supposition, the basic idea of the new method is to reproduce the original surface by reversing the process of sampling. As it is impossible to reproduce the original surface, the new method constructs a fitting surface to approximate the original surface in a local way. Reversing the process of sampling allows that the fitting surface has a better approximation precision.

The remaining part of the paper is arranged as follows. The basic idea of the new method is described in section 2. The construction of the fitting surface is discussed in section 3. The comparison of the new method with other methods is conducted in section 4. The conclusions are given in section 5.

2 Basic idea

Suppose that $\boldsymbol{P}$ is an image composed of $n \times n$ image elements, $P_{i,j}$ (the position marked by "•", as shown in Figure 1), $i, j = 1, 2, \ldots, n$. These image elements are generally sampling values, which can be regarded as taken from a continuous 2D original scene $F(x, y)$. For brevity, suppose that each element $P_{i,j}$ is sampled from a unit square, i.e,

$$P_{i,j} = \int_{-\frac{1}{2}}^{\frac{1}{2}} \int_{-\frac{1}{2}}^{\frac{1}{2}} w(x, y) F(x, y) dx dy,$$

where $w(x, y)$ is a weight function to make $P_{i,j}$ have good quality based on different applications.

The goal here is to construct a fitting surface $f(x, y)$ which approximates the original scene $F(x, y)$ with a quadratic polynomial approximation precision.

In many papers, the fitting surface $f(x, y)$ is typically implemented by convolving the image $P_{i,j}$ with

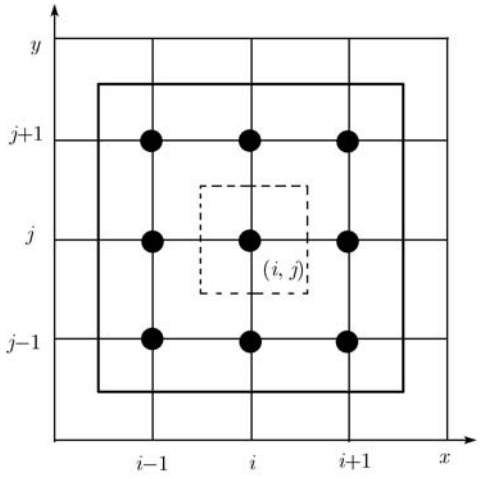

Figure 1 Image region.

a 2-D kernel $\kappa(x, y)$:

$$f(x,y) = \sum_{i=-\infty}^{+\infty} \sum_{j=-\infty}^{+\infty} P_{i,j}\kappa(x-i, y-j). \tag{1}$$

Here the key problem for (1) is to construct the kernel $\kappa(x, y)$.

In general, $\kappa(x, y)$ satisfies the following constraint:

$$\sum_{i=-\infty}^{+\infty} \sum_{j=-\infty}^{+\infty} \kappa(x-i, y-j) = 1.$$

Hence, $f(x, y)(1)$ is the blending combination of $P_{i,j}$, $i, j = 1, 2, \ldots, n$. Based on the approximation theory, if $P_{i,j}$ is a point on the original scene $F(x, y)$, i.e., $P_{i,j} = F(i, j)$, expression (1) could give good result. Unfortunately, $P_{i,j}$ is generally not a point on $F(x, y)$ in real applications, but a sampling value taken from a region of $F(x, y)$. Thus, expression (1) does not yield good result. To remedy this problem, one of the best ways is to resample the new image elements from $F(x, y)$, which requires $F(x, y)$ to be known. After $F(x, y)$ is known, we can easily resize the image by formulae similar to (2). Hence resizing the image $\mathbf{P}$ becomes a problem of constructing $F(x, y)$. In the following, we will discuss how to construct $F(x, y)$.

For brevity, suppose that $F(x, y)$ is defined on the region $[1/2, n + 1/2] \times [1/2, n + 1/2]$. Thus, each $P_{i,j}$, $i, j = 1, 2, \ldots, n$ is sampled from a unit square and satisfies the following condition:

$$P_{i,j} = \int_{i-\frac{1}{2}}^{i+\frac{1}{2}} \int_{j-\frac{1}{2}}^{j+\frac{1}{2}} w(x,y)F(x,y)dxdy. \tag{2}$$

For brevity, we let $w(x, y) = 1$ in this paper, the case that $w(x, y)$ is a function in general form will be studied in the future.

Note: $P_{i,j}$, $i, j = 1, 2, \ldots, n$ are integer, hence, (2) does not hold in general, but holds approximately.

Generally speaking, based on the image $\mathbf{P}$, it is hard or impossible to construct $F(x, y)$ exactly. Instead, we construct the surface $f(x, y)$ to fit $F(x, y)$. The basic idea for constructing the surface $f(x, y)$ can be described simply as below. On each region $[i-1.5, i+1.5] \times [j-1.5, j+1.5]$ (the square bounded by solid line), $i, j = 2, 3, \ldots, n-1$, as shown in Figure 1, a quadratic polynomial patch $f_{i,j}(x, y)$ is constructed, the fitting surface $f(x, y)$ is constructed by the weighted combination of $f_{i,j}(x, y)$, $i, j = 2, 3, \ldots, n-1$. In the following, we discuss the construction of $f_{i,j}(x, y)$, $i, j = 2, 3, \ldots, n-1$.

2.1 Constructing patch $f_{i,j}(x,y)$

The patch $f_{i,j}(x, y)$, $i, j = 2, 3, \ldots, n-1$ will be constructed so that it satisfies the following condition. If $F(x, y)$ in (2) is a quadratic polynomial and (2) holds, $f_{i,j}(x, y)$, $i, j = 2, 3, \ldots, n-1$ should reproduce

$F(x,y)$ exactly, so that the fitting surface $f(x,y)$ reproduces $F(x,y)$ exactly. In this case, the fitting surface $f(x,y)$ is known as having a quadratic polynomial approximation precision.

Let $v=x-i$, $w=y-j$, the quadratic polynomial patch $f_{i,j}(x,y)$ can be written as

$$\begin{aligned} f_{i,j}(x,y) = {} & \frac{v(v-1)}{2}\bar{F}_{i-1,j} + \frac{v(v+1)}{2}\bar{F}_{i+1,j} + \frac{w(w-1)}{2}\bar{F}_{i,j-1} + \frac{w(w+1)}{2}\bar{F}_{i,j+1} \\ & + (1-v^2-w^2)F_{i,j} + vw\bar{D}_{i,j}, \end{aligned} \tag{3}$$

where $F_{i,j}$, $\bar{F}_{i-1,j}$, $\bar{F}_{i+1,j}$, $\bar{F}_{i,j-1}$, $\bar{F}_{i,j+1}$ and $\bar{D}_{i,j}$ are unknowns to be determined.

We first discuss the determination of $F_{i,j}$, $\bar{F}_{i-1,j}$, $\bar{F}_{i+1,j}$, $\bar{F}_{i,j-1}$ and $\bar{F}_{i,j+1}$. With eq. (2), we have

$$\int_{k-\frac{1}{2}}^{k+\frac{1}{2}}\int_{l-\frac{1}{2}}^{l+\frac{1}{2}} f_{i,j}(x,y)dxdy = P_{i+k,j+l}, \qquad (k,l)=\{(0,0),(-1,0),(1,0),(0,-1),(0,1)\}. \tag{4}$$

We get

$$\frac{1}{24}\begin{bmatrix} 20 & 1 & 1 & 1 & 1 \\ -4 & 25 & 1 & 1 & 1 \\ -4 & 1 & 25 & 1 & 1 \\ -4 & 1 & 1 & 25 & 1 \\ -4 & 1 & 1 & 1 & 25 \end{bmatrix}\begin{bmatrix} F_{i,j} \\ \bar{F}_{i-1,j} \\ \bar{F}_{i+1,j} \\ \bar{F}_{i,j-1} \\ \bar{F}_{i,j+1} \end{bmatrix} = \begin{bmatrix} P_{i,j} \\ P_{i-1,j} \\ P_{i+1,j} \\ P_{i,j-1} \\ P_{i,j+1} \end{bmatrix}.$$

Its solution is

$$\begin{bmatrix} F_{i,j} \\ \bar{F}_{i-1,j} \\ \bar{F}_{i+1,j} \\ \bar{F}_{i,j-1} \\ \bar{F}_{i,j+1} \end{bmatrix} = \frac{1}{24}\begin{bmatrix} 28 & -1 & -1 & -1 & -1 \\ 4 & 23 & -1 & -1 & -1 \\ 4 & -1 & 23 & -1 & -1 \\ 4 & -1 & -1 & 23 & -1 \\ 4 & -1 & -1 & -1 & 23 \end{bmatrix}\begin{bmatrix} P_{i,j} \\ P_{i-1,j} \\ P_{i+1,j} \\ P_{i,j-1} \\ P_{i,j+1} \end{bmatrix}.$$

We now discuss the determination of $\bar{D}_{i,j}$. With eq. (2), we have

$$\int_{k-\frac{1}{2}}^{k+\frac{1}{2}}\int_{l-\frac{1}{2}}^{l+\frac{1}{2}} f_{i,j}(x,y)dxdy = P_{i+k,j+l}, \quad (k,l)=\{(-1,-1),(1,-1),(-1,1),(1,1)\}. \tag{5}$$

Then, we have the following equations:

$$\begin{aligned} &24\bar{D}_{i,j} + 25\bar{F}_{i-1,j} + \bar{F}_{i+1,j} + 25\bar{F}_{i,j-1} + \bar{F}_{i,j-1} - 28F_{i,j} = 24P_{i-1,j-1}, \\ &-24\bar{D}_{i,j} + \bar{F}_{i-1,j} + 25\bar{F}_{i+1,j} + 25\bar{F}_{i,j-1} + \bar{F}_{i,j+1} - 28F_{i,j} = 24P_{i+1,j-1}, \\ &-24\bar{D}_{i,j} + 25\bar{F}_{i-1,j} + \bar{F}_{i+1,j} + \bar{F}_{i,j-1} + 25\bar{F}_{i,j+1} - 28F_{i,j} = 24P_{i-1,j+1}, \\ &24\bar{D}_{i,j} + \bar{F}_{i-1,j} + 25\bar{F}_{i+1,j} + \bar{F}_{i,j-1} + 25\bar{F}_{i,j+1} - 28F_{i,j} = 24P_{i+1,j+1}. \end{aligned}$$

The value of $\bar{D}_{i,j}$ is defined by

$$\bar{D}_{i,j} = \frac{1}{4}(P_{i-1,j-1} + P_{i+1,j+1} - P_{i+1,j-1} - P_{i-1,j+1}). \tag{6}$$

Theorem 1. For an image $\mathbf{P}$ which is composed of $n\times n$ image elements, $P_{i,j}$, $i,j=1,2,\ldots,n$, if $P_{i,j}$ is defined by (2), the patch $f_{i,j}(x,y)$ has a quadratic polynomial approximation precision.

Proof. If $F(x,y)$ in (2) is a quadratic polynomial surface, the constructing process of $f_{i,j}(x,y)(3)-(6)$ show that $f_{i,j}(x,y)=F(x,y)$, $i,j=2,3,\ldots,n-1$ make (3)–(6) hold. As $f_{i,j}(x,y)$, $i,j=2,3,\ldots,n-1$ are unique, $f_{i,j}(x,y)=F(x,y)$, $i,j=2,3,\ldots,n-1$. This completes the proof of the theorem.

2.2 Modifying patch $f_{i,j}(x,y)$

By (3), one obtains five values, $F_{i,j}$, $\bar{F}_{i-1,j}$, $\bar{F}_{i+1,j}$, $\bar{F}_{i,j-1}$, $\bar{F}_{i,j+1}$, which can be regarded as the approximation of $F(x,y)$ at points $(i+k,j+l)$, $(k,l)=\{(0,0),(-1,0),(1,0),(0,-1),(0,1)\}$, respectively. Based on approximation theory and our experiments, among the five values, $F_{i,j}$ has generally the better approximation than $\bar{F}_{i-1,j}$, $\bar{F}_{i+1,j}$, $\bar{F}_{i,j-1}$ and $\bar{F}_{i,j+1}$ do. To have better approximation, $f_{i,j}(x,y)$ (3) is modified by

$$\begin{aligned} f_{i,j}(x,y) = {} & \frac{v(v-1)}{2}F_{i-1,j} + \frac{v(v+1)}{2}F_{i+1,j} + \frac{w(w-1)}{2}F_{i,j-1} + \frac{w(w+1)}{2}F_{i,j+1} \\ & + (1-v^2-w^2)F_{i,j} + vwD_{i,j}. \end{aligned} \tag{7}$$

In the following, we first discuss the determination of $F_{i,j}$, $i,j=1,2,3,\ldots,n$, then, the determination of $D_{i,j}$ in (7), $i,j=2,3,\ldots,n-1$.

The values of $F_{i,j}$, $i,j=1,2,3,\ldots,n$ are determined by the following procedure:

• For $i,j=2,3,\ldots,n-1$, $F_{i,j}$ is computed by $f_{i,j}(x,y)$ (3) at $(x,y)=(i,j)$.

• For $j=1,2,\ldots,n$, $F_{1,j}$ and $F_{n,j}$ are defined by $f_{i,j}(x,y)$ (3) with $F_{1,j}=f_{2,j}(1,j)$ and $F_{n,j}=f_{n-1,j}(n,j)$.

• For $i=2,3,\ldots,n-1$, $F_{i,1}$ and $F_{i,n}$ are defined by $f_{i,j}(x,y)$ (3) with $F_{i,1}=f_{i,2}(i,1)$ and $F_{i,n}=f_{i,n-1}(i,n)$.

It is easy to know that if $F(x,y)$ in (2) is a quadratic polynomial, then, for $i,j=2,3,\ldots,n-1$, its second blend partial derivative can be expressed by

$$D_{i,j} = \frac{F_{i-1,j-1}+F_{i+1,j+1}-F_{i+1,j-1}-F_{i-1,j+1}}{4}. \tag{8}$$

2.3 Discussion

On the region $[i-1,j-1]\times[i+1,j+1]$, $f_{i,j}(x,y)$ defined by (7) should satisfy $0\leqslant f_{i,j}(x,y)\leqslant 255$, so that the fitting surface $f(x,y)$ that will be constructed in section 3 satisfies $0\leqslant f(x,y)\leqslant 255$. If $f_{i,j}(x,y)$ (7) has negative values, we could remove them by the following way. Assume that $f_{i,j}(x,y)$ reaches its minimum value $f_{i,j}(x_p,y_p)$ at point (x_p,y_p) on the region $[i-1,j-1]\times[i+1,j+1]$. If the value $f_{i,j}(x_p,y_p)$ is negative, $f_{i,j}(x,y)$ should be redefined by

$$f_{i,j}(x,y)+|f_{i,j}(x_p,y_p)|. \tag{9}$$

For the case of the maximum value of $f_{i,j}(x,y)>255$, assume that $f_{i,j}(x,y)$ reaches its maximum value $f_{i,j}(x_c,y_c)$ at point (x_c,y_c) on the region $[i-1,j-1]\times[i+1,j+1]$, i.e., $f_{i,j}(x_c,y_c)>255$, $f_{i,j}(x,y)$ should be redefined by

$$255\times f_{i,j}(x,y)/f_{i,j}(x_c,y_c). \tag{10}$$

3 Constructing fitting surface $f(x,y)$

In this section, we will discuss how to construct the fitting surface $f(x,y)$ using the quadratic polynomial patch $f_{i,j}(x,y)$, $i,j=2,3,\ldots,n-1$. On each region $[i,i+1]\times[j,j+1]$, $i,j=1,2,\ldots,n-1$, a bi-cubic patch $B_{i,j}(x,y)$ is constructed, all $B_{i,j}(x,y)$, $i,j=1,2,\ldots,n-1$, are put together to form the fitting surface $f(x,y)$.

On the region $[i,i+1]\times[j,j+1]$, $i,j=2,3,\ldots,n-2$, the bi-cubic patch $B_{i,j}(x,y)$ is constructed by the combination of $f_{i,j}(x,y)$, $f_{i+1,j}(x,y)$, $f_{i,j+1}(x,y)$ and $f_{i+1,j+1}(x,y)$, i.e, $B_{i,j}(x,y)$ is defined by

$$\begin{aligned} B_{i,j}(x,y) = {} & w_{i,j}(x,y)f_{i,j}(x,y) + w_{i+1,j}(x,y)f_{i+1,j}(x,y) + w_{i,j+1}(x,y)f_{i,j+1}(x,y) \\ & + w_{i+1,j+1}(x,y)f_{i+1,j+1}(x,y), \end{aligned} \tag{11}$$

where

$$w_{i,j}(x,y)=(1-v)(1-w), \quad w_{i+1,j+1}(x,y)=vw,$$

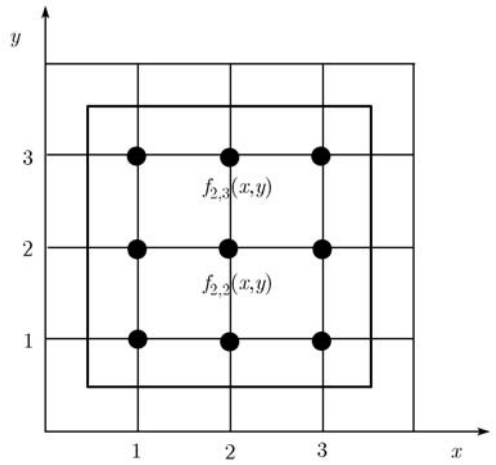

Figure 2 $B_{1,1}(x,y)$ defined by $f_{2,2}(x,y)$.

$$w_{i,j+1}(x,y) = (1-v)w, \quad w_{i+1,j}(x,y) = v(1-w)$$

are weight functions with $v = x - i$, $w = y - j$.

Now, we discuss the construction of the bi-cubic patches on the boundary of the region. The patches on the boundary are $B_{1,j}(x,y)$ and $B_{n-1,j}(x,y)$, $j = 1,2,\ldots,n-1$, $B_{i,1}(x,y)$ and $B_{i,n-1}(x,y)$, $i = 2,3,\ldots,n-2$. As symmetry, we only discuss the construction of $B_{1,j}(x,y)$, $j = 1,2,\ldots,n-1$, rest cases can be handled similarly. The $B_{1,1}(x,y)$ and $B_{1,n-1}(x,y)$ are defined by $f_{2,2}(x,y)$ and $f_{2,n-1}(x,y)$, respectively, as shown in Figure 2. For $j = 2,3,\ldots,n-2$, $B_{1,j}(x,y)$ is defined by

$$B_{1,j}(x,y) = f_{2,j}(x,y)(1-w) + f_{2,j+1}(x,y)w. \tag{12}$$

Based on Theorem 1 and the definition of $B_{i,j}(x,y)$ (11) and (12), it is easy to get the following theorem.

Theorem 2. If $P_{i,j}$ is defined by (2), the fitting surface $f(x,y)$ has a quadratic polynomial approximation precision.

4 Experiments

In this section, we will compare the efficiency of the new method with Bi-cubic method [4] and Separable PCC(optimized) [16]. For brevity, the new method, Bi-cubic method, and Separable PCC(optimized) are denoted by Md1, Md2, and Md3, respectively. The comparison is carried out on two sets of examples. The first set of examples uses a continuous function $F(x)$ to compare the precision of Md1 and Md2. Md3 is not compared as it cannot be used to construct a curve directly. The function $F(x)$ is defined by

$$\begin{aligned} F(x) = 2.5 + (&0.5\cos(1000x) + \cos(400x) + \cos(600x) + \cos(500x) + 0.4\cos(800x) \\ &+ 1000(x-0.2)(x-0.25)(x-0.3))/2. \end{aligned}$$

The sampling points P_i, $i = 0,1,2,\ldots,199$ are defined by

$$P_i = \int_{\frac{i}{200}}^{\frac{i+1}{200}} F(x)dx.$$

Let $E(x)$ and $G(x)$ be two curves constructed by Md2 and Md1, respectively, which can be regarded as the approximation to $F(x)$. Let $e_1(x) = F(x) - E(x)$ and $e_2(x) = F(x) - G(x)$ be the two error curves. The plots of the two error curves are given in Figure 3. In Figure 3, the curve on the top is the plot of $F(x)$, the symbols "$\circ$" on the curve are sampling points, P_i, $i = 0,1,2,\ldots,199$; the curve in the middle

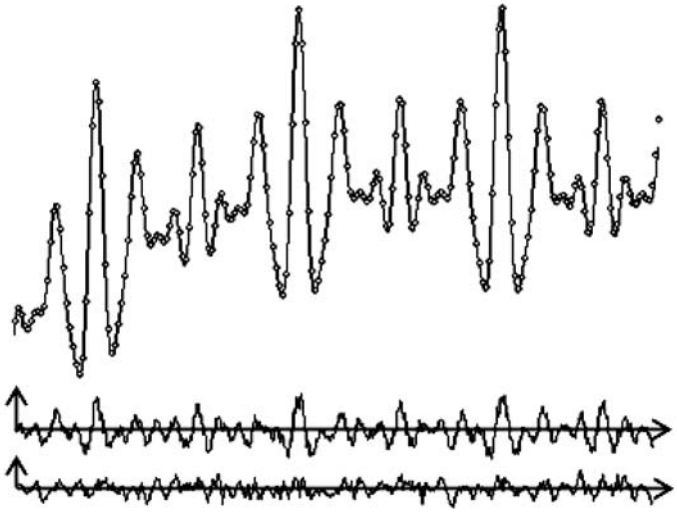

Figure 3 Original curve and two error curves.

Figure 4 Four images for comparison. (a) Goldhill; (b) Lenna; (c) peppers; (d) boat.

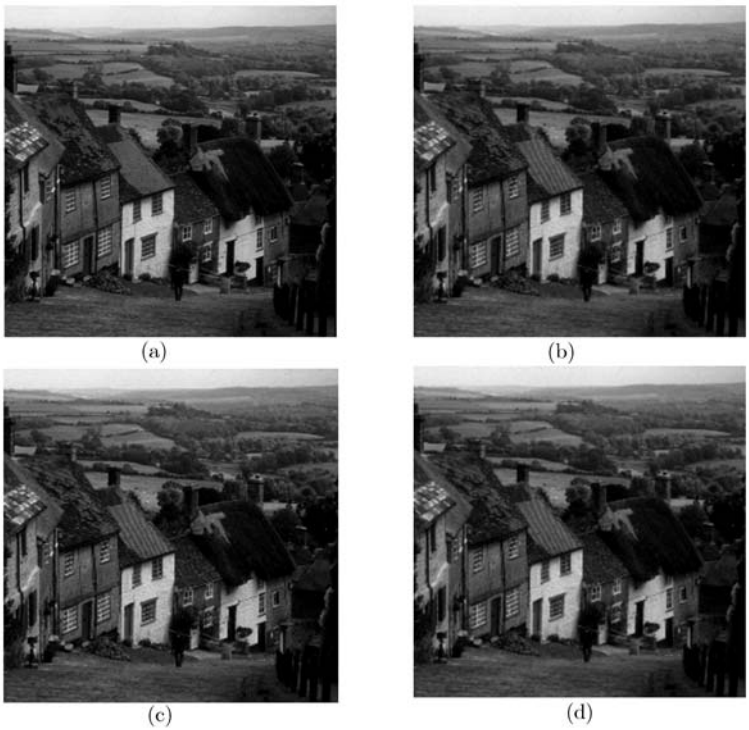

Figure 5 Enlarged Goldhill image (256×256 to 512×512). (a) Original image; (b) image by new method; (c) image by Bi-cubic method; (d) image by PCC.

is the plot of $e_1(x)$; the curve at the bottom is the plot of $e_2(x)$, where the maximum absolute errors of $e_1(x)$ and $e_2(x)$ are 0.039457 and 0.013320, respectively. Figure 3 shows that $G(x)$ has better approximation to $F(x)$ than $E(x)$ does.

In the second set of examples, the efficiency of Md1 is compared with Md2 and Md3 using the four standard images shown in Figure 4. These four standard images are used often for comparing the efficiency of image processing methods. The comparison is carried out by enlarging the four standard images with the resolving powers 256×256 and 128×128, respectively. The enlarged images are compared with the four standard images with the resolving power 512×512.

We first compare the quality of the images produced using the three methods by vision. One of the comparison results is shown in Figure 5, where, image (a) is the original image with size 512×512, and images (b), (c), and (d) with size 512×512 are enlarged images, which are created by Md1, Md2 and Md3 from the 256×256 image, respectively.

Then, the images enlarged by the three methods are compared in terms of the fidelity [23] defined by

$$p = 1 - \frac{\sum\sum |R_{i,j} - P_{i,j}|}{\sum\sum P_{i,j}} \tag{13}$$

and PSNR (peak signal to noise ratio) defined by

$$\text{PSRN} = 10 \lg_{10} \left(\frac{n \times n \times 255 \times 255}{\sum_{j=1}^{n} \sum_{i=1}^{n} (R_{i,j} - P_{i,j})^2} \right), \tag{14}$$

which are normalized measures for testing the image quality, where $P_{i,j}$ is the accurate image element, and $R_{i,j}$ is the enlarged image element produced by one of the three methods.

The fidelity and the PSRN of the three methods applied to the four images (size 256×256) are given in Table 1. The fidelity and the PSRN of the three methods applied to the four images (size 128×128) are given in Table 2.

Figure 5 and Tables 1 and 2 show that the new method gets better results. The new method has been compared with the two methods on other images. The results are similar to the ones as shown in Figure 5 and Tables 1 and 2.

5 Conclusions

In this paper, we present a new method for the image fitting surface construction. The new method is useful in image processing, especially in image resizing. The new method is based on the fact that the given data points of an image can be regarded as being sampled from an original scene that can be approximated by a piecewise defined surface known as original surface. The new method constructs the

Table 1 Fidelity and PSRN of the three methods (image size: 256×256)

Image	Fidelity			PSRN		
	Md1	Md2	Md3	Md1	Md2	Md3
Goldhill	0.945	0.936	0.924	28.45	27.32	27.49
Boat	0.970	0.959	0.959	31.40	28.42	28.42
Lenna	0.970	0.959	0.959	31.44	28.55	28.62
Peppers	0.972	0.963	0.963	34.02	30.72	30.71

Table 2 Fidelity and PSRN of the three methods (image size: 128×128)

Image	Fidelity			PSRN		
	Md1	Md2	Md3	Md1	Md2	Md3
Goldhill	0.937	0.911	0.911	27.72	24.76	24.75
Boat	0.947	0.926	0.926	26.48	23.29	23.32
Lenna	0.957	0.931	0.931	27.71	24.03	24.02
Peppers	0.957	0.933	0.933	29.59	24.92	24.92

fitting surface locally by piecewise bi-cubic polynomial patches formed by the combination of the four quadratic polynomial patches. The fitting surface can be regarded as an approximation of the original surface, approximate the original surface with a quadratic polynomial interpolation precision under constraint (2). The comparison results also indicate that when the new method is used to construct the fitting surface, the resized images resampled from the fitting surface have high precision and good quality.

Unlike the existing methods, the new method constructs the fitting surface of the original surface by reversing the process of sampling. This is a new idea for constructing the fitting surface to image. It makes the procedure of constructing the fitting surface a procedure of reversing the process of sampling. In this paper, we use piecewise quadratic polynomials to construct the fitting surface. In the following work, we will conduct research on further improving the approximation precision by investigating other forms of functions to construct the fitting surface.

Acknowledgements

This work was supported by the National Basic Research Program of China (Grant No. 2006CB303102), and the National Natural Science Foundation of China (Grant Nos. 60673003, 60933008), Shandong Province Natural Science Foundation (Grant No. Z2006G05).

References

1 Gonzalez R C, Gonzalez R C, Woods R E. Digital Image Processing. Reading, MA: Addision-Wesley, 1992
2 Maeland E. On the comparison of interpolation methods. IEEE Trans Med Imag, 1988, 7: 213–217
3 Parker J A, Kenyon R V, Troxel D E. Comparison of interpolating methods for image resampling. IEEE Trans Med Imag, 1983, MI-2: 31–39
4 Keys R G. Cubic convolution interpolation for digital image processing. IEEE Trans Acoust Speech Signal Proc, 1981, 29: 1153–1160
5 Hsieh H, Andrews H C. Cubic splines for image interpolation and digital filtering. IEEE Trans Acoust Speech Signal Proc, 1981, 26: 508–517
6 Park S K, Schowengerdt R A. Image reconstruction by parametric cubic convolution. Comput Vision Graph Image Proc, 1983, 23: 258–272
7 Meijering E H W, Niessen W J, Viergever M A. Piecewise polynomial kernels for image interpolation: A generalization of cubic convolution. In: Proc IEEE Int Conf Image Processing, Kobe, Japan, 1999. 647–651
8 Unser M, Aldroubi A, Eden M. Fast B-spline transforms for continuous image representation and interpolation. IEEE Trans Patt Anal Mach Intell, 1991, 13: 277–285
9 Munoz A, Blu T, Unser M. Least-squares image resizing using finite differences. IEEE Trans Image Proc, 2001, 10: 1365–1378
10 Pumar M A. Zooming of terrain imagery using fractal-based interpolation. Comput Graphic, 1996, 20: 171–176
11 Unser M, Aldroubi A, Eden M. Enlargement or reduction of digital images with minimum loss of information. IEEE Trans Image Proc, 1995, 4: 247–258
12 Lehmann T M, Gonner C, Spitzer K. Survey: interpolation methods in medical processing. IEEE Trans Med Imag, 1999, 18: 1049–1075
13 Battiato S, Gallo G, Stanco F. A locally adaptive zooming algorithm for digital images. Image Vision Comput, 2002, 20: 805–812
14 Chang C C, Chou Y C, Yu Y H, et al. An image zooming technique based on vector quantization approximation. Image Vision Comput, 2005, 23: 1214–1225
15 Reichenbach S E, Geng F. Two-dimensional cubic reichenbach convolution. IEEE Trans Image Proc, 2003, 12: 857–865
16 Shi J, Reichenbach S E. Image interpolation by two-dimensional parametric cubic convolution. IEEE Trans Image Proc, 2006, 15: 1857–1870
17 Li X, Orchard M T. New edge-directed interpolation. IEEE Trans Image Proc, 2001, 10: 1521–1527
18 Zhang X, Wu X. Image interpolation by adaptive 2-D autoregressive modeling and soft-decision estimation. IEEE Trans Image Proc, 2008, 17: 887–896
19 Avidan S, Shamir A. Seam carving for content-aware image resizing. ACM Trans Graph (SIGGRAPH), 2007, 26: 10–18
20 Rubinstein M, Shamir A, Avidan S. Improved seam carving for video retargeting. ACM Trans Graph (SIGGRAPH), 2008, 27: 1–9
21 Zhang Y F, Hu S M, Martin R R. Shrinkability maps for content-aware video resizing. Comput Graph Forum, 2008, 27: 1797–1804
22 Huang H, Fu T N, Rosin P L, et al. Real-time content-aware image resizing. Sci China Ser F-Inf Sci, 2009, 52: 172–182
23 Linfoot E H. Transmission factors and optical design. J Optic Society America, 1956, 46: 740–752